OPEN ACCESS

# OPTIMIZING FUNCTIONALLY GRADED MATERIALS PLATE TOPOLOGY FOR THERMAL-AERODYNAMIC FLUTTER RESISTANCE

*Mohamed E Fayed[1], Mohammad Tawfik[2,3], A A El Desouky[1], Ehab Ali[1] and Mourad S Semary[1,4]*
*[1]Basic Engineering Sciences Department, Benha Faculty of Engineering, Benha University, Egypt.*
*[2]Academic Director, Academy of Knowledge, Egypt.*
*[3]Professor, Faculty of Engineering, Emirates Aviation University, UAE.*
*[4]Basic Sciences Department, Faculty of Engineering, Badr University in Cairo BUC, Cairo 11829, Egypt.*
*Email: melsayed@bhit.bu.edu.eg*

**Abstract** - This study investigates the optimization of functionally graded Nickel-Aluminum plates under combined thermal and aerodynamic loading conditions, with a specific focus on panel flutter resistance. The study implements polynomial functions for material distribution optimization, contributing to the ongoing research in aerospace structural design methodologies. Through finite element analysis implemented in MATLAB with a 9×9 node distribution, we examined plates with clamped boundary conditions on all edges, achieving significant improvements in performance characteristics compared to homogeneous reference cases.

**Keywords**: Functionally Graded Materials, Panel Flutter, Finite Element Analysis, Topology Optimization, Nickel Distribution.

## 1. Introduction

The pursuit of lightweight yet robust structures in aerospace engineering has led to significant advancements in materials and design methodologies. Functionally Graded Materials (FGMs) have emerged as a promising solution, offering the ability to tailor material properties across a structure to meet specific performance requirements. In the context of aircraft panels and other aerospace applications, the challenge of maintaining structural integrity under combined thermal and aerodynamic loading is particularly critical.

Panel flutter, a self-excited oscillation caused by the interaction between aerodynamic forces and the elastic properties of a structure, remains a significant concern in high-speed flight. The ability to optimize the topology of FGM plates to enhance flutter resistance represents a cutting-edge approach to addressing this challenge. By strategically distributing materials within a plate, it is possible to create structures that are more resilient to the complex loading conditions experienced in aerospace environments.

This study focuses on the topology optimization of FGM plates to maximize flutter resistance under thermal and aerodynamic loading.

Utilizing finite element analysis implemented in MATLAB, we explore various material distribution patterns within a plate measuring 1.0 x 1.0 x 0.001 m. The investigation considers both quadratic and polynomial distribution functions to determine the optimal configuration for clamped boundary conditions.

The significance of this research lies in its potential to inform the design of next-generation aerospace structures. By developing a methodology for optimizing FGM plates, we aim to contribute to the creation of more efficient, durable, and safe aircraft components capable of withstanding the extreme conditions encountered in high-speed flight.

An extensive research effort has focused recently on theoretically and numerically analyzing stability and flutter phenomena in panels under aerodynamic, thermal, acoustic and multifunctional loads to enable optimization.

[1] developed finite element modeling to evaluate the effects of functionally graded materials and constituents on thermal buckling and nonlinear flutter in panels, finding silicon nitride-Nickel reinforcement improves temperature-dependent response while spatial gradations and mixing ratios significantly influence static and dynamic behavior. [2] established related formulation specialized for efficient flutter and buckling analysis, where Nickel-




*https://doi.org/10.17683/ijomam/issue19*

silicon nitride blending tunes stability and graded variations optimize integrity, vibrations and aerodynamic performance.

[3] put forward symbolic derivatives and optimization for variability quantification in free vibration of functionally graded plates, demonstrating higher-order reliability methods agree well with Monte Carlo simulations. The approach provides a basis to extend robustness-based design optimization to multiple performance metrics leveraging graded materials. [4] focused on thermal flutter in graded panels, determining increased ceramic volume fraction elevates flutter resistance as well as high-cycle fatigue driving loads. Studies [5, 6] explored nonlinear finite element analysis and time-domain simulations to reveal complex trade-offs between post-buckling, forced response and fatigue life predictions under combined thermal-acoustic loads.

[7] proposed a polynomial expansion-based method for multi-dimensional optimization of functionally graded materials (FGMs) composition, offering greater design flexibility compared to power-law or exponential-law methods. Applied to an Aluminum plate reinforced with silicon carbide nanoparticles, the method demonstrated significant material savings of 20-80% in reinforcement volume while maintaining or improving mechanical performance, particularly beneficial for aerospace applications due to minimal weight increase.[8] developed a meshfree method using radial basis functions and collocation techniques for analyzing the buckling of functionally graded material (FGM) thin plates with in-plane material inhomogeneity. The study demonstrated that material inhomogeneity significantly affects buckling loads and mode shapes, suggesting that it can be exploited to optimize in-plane stress distribution and prevent buckling in thin plates, which is valuable for tailoring and designing FGMs.[9-12] provided a comprehensive review of functionally graded materials (FGMs) and structures, focusing on their structural responses under various conditions and highlighting different fabrication techniques. The study concluded that while FGMs show great potential in aerospace and healthcare applications, further research is needed to improve fabrication techniques, refine theoretical models, and explore new applications, particularly in the medical field. highlights the challenges of solving 3D analytical models due to their complexity and suggests that improved 2D theoretical models, which offer similar accuracy at lower computational costs, should be further explored.

[13] explored the impact of material gradation and layout on the overall stiffness of functionally graded structures using continuous topology optimization with symmetry and pattern repetition constraints. The study demonstrated that their approach could reproduce results previously obtained through homogenization techniques for cellular materials, suggesting potential applications in representing microstructures of graded cellular materials and opening avenues for further research in material design, including meta-materials and hybrid materials.[14] investigated the dynamic behavior of moderately thick 2D Functionally Graded (FG) cylindrical shells on a Winkler-Pasternak elastic foundation using the First-order Shear Deformation Theory (FSDT) and the Generalized Differential Quadrature (GDQ) method. The research found that 2D-FG cylindrical shells exhibited higher natural frequencies compared to 1D-FG shells, and that various factors such as material distribution, shell geometry, and foundation characteristics significantly influenced the vibration characteristics of these structures.

[15] conducted a pioneering three-dimensional free vibration analysis of two-dimensional functionally graded fiber-reinforced (2-D FGFR) curved panels with various boundary conditions, introducing a novel six-parameter power-law distribution for fiber volume fractions. The study demonstrated that this 2-D FGFR approach offers designers greater flexibility in tailoring structural properties compared to conventional one-dimensional FGFR, allowing for more precise control over frequency parameters and vibrational displacements, which can be optimized for specific multi-functional requirements in different applications.[16] developed a methodology for two-dimensional simulation and optimization of volume fraction distribution in two-phase functionally graded materials (FGMs) for thermomechanical processes, using the element-free Galerkin method and a real-coded genetic algorithm. The study demonstrated the effectiveness of this approach by optimizing FGM compositions in two model problems, achieving significant improvements in thermomechanical performance compared to linearly graded materials, such as a 55.9% reduction in peak residual stress for a Ni/Al2O3 component and superior stress and temperature management in an Al/zirconia component while reducing overall ceramic content.[17-18] have developed efficient frameworks for optimizing material properties and structural designs. Introduced a compact MATLAB code for designing materials with extreme properties, simplifying the numerical implementation using an energy-based homogenization approach. and proposed a level set-based method for simultaneously optimizing material properties and structural topology in functionally graded structures, effectively integrating volume fraction and structural boundaries into a unified design process.[19] presented an approach to model and process functionally graded material (FGM) objects by integrating material information with geometry information in a heterogeneous solid model. It

utilized a CAD system for geometry modeling and adopted the STEP standard exchange format for exchanging geometric information. Material information was represented using a group of distance functions, allowing for easy modification of material distribution without altering the object's geometry. The processing of FGM models involved discretizing the continuous material distribution in 2D layers rather than 3D space, which significantly reduced memory usage.

## 2. Mathematical Model Using Super Elements

The proposed methodology combines finite element analysis with evolutionary optimization techniques to analyze and optimize functionally graded materials (FGMs). This integrated approach leverages super elements for computational efficiency while maintaining solution accuracy.

The finite element method (FEM) forms the foundation of this model, with super elements replacing standard elements to enhance computational performance.[21] These super elements incorporate higher-order shape functions, allowing for a reduction in the total number of elements while maintaining solution precision. The displacement field $u(x,y)$ within a super element is represented as a summation of shape functions and nodal displacements:

$$u(x,y) = \sum_{i}^{n} N_i(x,y)u_i \tag{1}$$

where $N_i\,(x,y)$ are higher-order shape functions derived from polynomial expansions, and u_i are the nodal displacement values. These shape functions are designed to satisfy $C1$ or $C2$ continuity requirements, ensuring smooth transitions across element boundaries.

### 2.1 Nonlinear Strain-Displacement Relation

The in-plane strains and curvatures, based on the von Kármán moderately large deflection, are given by:

$$\begin{Bmatrix}\epsilon_x\\ \epsilon_y\\ \gamma_{xy}\end{Bmatrix} = \begin{Bmatrix}u_x\\ v_y\\ u_y+v_x\end{Bmatrix} + \frac{1}{2}\begin{Bmatrix}w_x^2\\ w_y^2\\ 2w_xw_y\end{Bmatrix} - z\begin{Bmatrix}w_{xx}\\ w_{yy}\\ 2w_{xy}\end{Bmatrix} \tag{2}$$

or, in compact form,

$$\{\epsilon\} = \{\epsilon_m\} + \frac{1}{2}\{\epsilon_\theta\} + \{\epsilon_b\} \tag{3}$$

where:

$\{\varepsilon_m\}$ is the membrane linear strain vector, $\{\varepsilon_\theta\}$ is the membrane nonlinear strain vector, $\{\varepsilon_b\}$ is the bending strain vector, $\{u,v\}$ are the in-plane displacements and $\{w,w_x,w_y,w_{xy}\}$ are the transverse displacements.

### 2.2 Stress–Strain Relationship of an FGMs Panel

The stress–strain relations for material that has changing properties in the x and y-directions can be expressed as follows:

$$\{\sigma\} = \begin{Bmatrix}\sigma_x\\ \sigma_y\\ \tau_{xy}\end{Bmatrix} = [Q(x,y)]\{\varepsilon\} \tag{4}$$

Where: $\{\sigma\}$ is the in-plane stress vector, $[Q(x,y)]$ is the stiffness matrix. The equilibrium relations may be expressed as:

$$\begin{Bmatrix}N\\ M\end{Bmatrix} = \begin{bmatrix}[A] & [0]\\ [0] & [D]\end{bmatrix}\begin{Bmatrix}\varepsilon\\ \kappa\end{Bmatrix} - \begin{Bmatrix}\{N_T\}\\ \{M_T\}\end{Bmatrix} \tag{5}$$

Where:

$$([A],[D]) = \iint_A\ [Q(x,y)](1,z^2)dz$$

$$[\mathrm{Q}(x,y)] = \begin{bmatrix}\frac{E(x,y)}{1-\nu^2(x,y)} & \frac{\nu(x,y)E(x,y)}{1-\nu^2(x,y)} & 0\\ \frac{\nu(x,y)E(x,y)}{1-\nu^2(x,y)} & \frac{E(x,y)}{1-\nu^2(x,y)} & 0\\ 0 & 0 & \frac{E(x,y)}{2[1+\nu(x,y)]}\end{bmatrix}$$

Where: $[A],[D]$ are the stiffness matrices, $\{N\},\{M\}$ are the resultant vectors of the in-plane force, moment $\{N_T\},\{M_T\}$ are the in-plane thermal load and thermal bending moment, E is the modulus of elasticity and $\nu$ is the Poisson ratio.

### 2.3 Aerodynamic Loading

The first-order quasi-steady piston theory for supersonic flow states that:

$$P_a = -\left(\frac{g_a}{\omega_0}\frac{D_{11}}{a^4}\frac{\partial w}{\partial t} + \lambda\frac{D_{11}}{a^3}\frac{\partial w}{\partial x}\right) \tag{6}$$

With

$$\mathrm{q} = \rho V^2/2, \qquad \beta = \sqrt{M_\infty^2 - 1} \qquad g_a = \frac{\rho_a V(M_\infty^2-2)}{\rho h\omega_0\beta^3}$$

$$\lambda = \frac{2qa^3}{\beta D_{11}} \qquad \omega_o = \left(\frac{D_{11}}{\rho h a^4}\right)^{\frac{1}{2}} \qquad D_{11} = \frac{Eh^3}{12(1-\nu^2)}$$

Where:

$P_a$ is the aerodynamic loading. $V$ is the velocity of airflow. $M_\infty$ is the Mach number. $q$ is the dynamic pressure. $\rho_a$ is the air mass density. $g_a$ is non-dimensional aerodynamic damping.

$\lambda$ is non-dimensional aerodynamic pressure. $D_{11}$ is the first entry of the flexural stiffness matrix $[D]$.

$a$ is the panel length in the flow direction, $\omega_0$ is the frequency and $\beta$ is the solidity ratio.

## 2.4 Equation of Motion

The equation of motion for functionally graded material involves predicting both the buckling response and post-buckling deformations. As outlinedby [22], this entails a multi-step process using the finite element method.

This direct coupled approach between linear buckling and geometrically nonlinear post-buckling analysis provides an efficient simulation procedure for resolving panel can be obtained as:

$$[M]\{\ddot{W}\}+[G]\{\dot{W}\}+([K]-[K_T]+\lambda[A_a]+\frac{1}{2}[N_1]+\frac{1}{3}[N_2])\{W\}=\{P_T\} \quad (7)$$

Where:
$[M]$ is the mass matrix, $[G]$ is the aerodynamic damping matrix, $[K]$ is the linear stiffness matrix, $[K_T]$ is the thermal geometric stiffness matrix, $[A_a]$ is the aerodynamic stiffness, $[N_1]$ is the first order nonlinear stiffness matrix and $[N_2]$ is the second order nonlinear stiffness matrix.

Separating equations (6) into lateral and transverse directions, we obtain the following two equations.

$$[M_b]\{\ddot{W}_b\}+\frac{g_a}{\omega_0}[G]\{\dot{W}_b\}+\left[[K_b]-[K_T]+\frac{\lambda}{a^3}[A_a]+\frac{1}{2}[N1_{nm}]+\frac{1}{3}[N2_b]\right]\{W_b\}=\{P_{b\Delta T}\}+\{P_b(t)\} \quad (8)$$

$$[M_m]\{\ddot{W}_m\}+[K_m]\{W_m\}=\{P_{m\Delta T}\} \quad (9)$$

Where:
suffixes $b, m$ and $nm$, are the bending, membrane and the nonlinear terms.
$\{P_b\ (t)\}$ is the external load vector, $\{P_{b\Delta T}\}$ is the thermal load vector.

## 2.5 Static Aerothermal Buckling

The solution procedure using the Newton–Raphson method for the aerothermal post-buckling analysis of a functionally graded material plate is presented as follows.

Introducing the function $\{\Psi(W)\}$ to,

$$\{\Psi(W)\}=\left([K]-[K_T]+\lambda[A_a]+\tfrac{1}{2}[N_1]+\tfrac{1}{3}[N_2]\right)\{W\}-\{P_T\}=0 \quad (10)$$

Eq. (9) can be written in the form of a truncated Taylor series expansion as:

$$\{\Psi(W+\delta W)\}=\{\Psi(W)\}+\frac{d\{\Psi(W)\}}{dW}\{\delta W\}\cong 0 \quad (11)$$

where:

$$\frac{d\{\Psi(W)\}}{dW}=[K]-[K_T]+\lambda[A_a]+\frac{1}{2}[N_1]+\frac{1}{3}[N_2]=[K_{tan}] \quad (12)$$

Thus, the Newton–Raphson iteration procedure for the determination of the post-buckling deflection can be expressed as follows:

$$\{\Psi(W)\}_i=([K]-[K_T]+\lambda[A_a]+\frac{1}{2}([N_1])_i+\frac{1}{3}([N_2])_i)\{W\}_i-\{P_T\}$$

Convergence occurs in the preceding procedure when the maximum value of $\{\delta W\}_{i+1}$becomes less than a given tolerance $\boldsymbol{\varepsilon_{tol}}$ $(\boldsymbol{i.e.,\max|\{\delta W\}_{i+1}|\varepsilon_{tol}).[N_1]=0}$ for the symmetric geometry and deformation pattern

## 2.6 Panel Flutter Under Thermal Effect

In this section, the procedure of determining the critical non-dimensional dynamic pressure under the presence of thermal loading can be reduced for the solution of the linear (pre-buckling and pre-flutter) problem to the following equation:

$$[M]\{\ddot{W}\}+[G]\{\dot{W}\}+([K]-[K_T]+\lambda[A_a]+[N_2])\{W\}=0 \quad (13)$$

Now assume the deflection function of the transverse displacement $\{W_B\}$ to be in the form of:

$$\{W_B\}=\bar{c}\{\Phi_B\}e^{\Omega t} \quad (14)$$

Where:
$\Omega=\alpha+i\omega$ is the complex panel motion parameter ($\alpha$ is the damping ratio and $\omega$ is the frequency), $\bar{c}$ is the amplitude of vibration, and $\{\Phi_B\}$ is the mode shape.

Substituting Eq. (12) into Eq. (13), the generalized eigenvalue problem can be obtained as

$$\bar{c}[-k(M_B)+(\bar{K}_B)]\{\Phi_B\}e^{\Omega t}=\{0\} \quad (15)$$

Where:
$[G_B]=\omega_0\ g_a\ [M_B\ ]$, and $k$ is the non-dimensional eigenvalue given by:

$$k=-\Omega^2-\omega_0 g_a\Omega \quad (16)$$

From Eq. (14), we can write the generalized eigenvalue problem:

$$[-k(M_B)+(\bar{K}_B)]\{\Phi_B\}=\{0\} \quad (17)$$

Where:

$k$ is the eigenvalue and $\Phi_B$ is the mode shape, with the characteristic equation written as:

$$|-k(M_B) + (\bar{K}_B)| = \{0\} \quad (18)$$

Given that the values of $k$ are real for all values of below the critical value, an iterative solution can be used to determine the critical non-dimensional dynamic pressure $\lambda_{cr}$.

## 3. The Volume Fraction Distribution Methods

The optimization of material distribution within this super element-based model is achieved through a genetic algorithm $(GA)$. This evolutionary approach begins with an initial population of potential solutions, each representing a unique material distribution over the $2D$ plate.

### 3.1 The Volume Fraction Distribution Methods

In this study, four different mathematical approaches were implemented to distribute the volume fraction of materials across the plate in both x and y directions. Each method offers distinct characteristics in controlling the material distribution pattern.

#### 3.1.1 Linear Distribution

The simplest distribution method implemented is the linear function, where the volume fraction varies linearly across the plate:

$$V(x,y) = ax + by + c \quad (19)$$

Where:

$V(x,y)$ represents the volume fraction at any point $(x,y)$, and $a, b$, and $c$ are coefficients determining the gradient of material distribution.

#### 3.1.2 Quadratic Distribution

A more complex distribution pattern was achieved using a quadratic function, allowing for curvilinear variation of material properties:

$$V(x,y) = ax^2 + by^2 + cxy + dx + ey + f \quad (20)$$

where a,b,c,d,e, and f are coefficients controlling the quadratic surface shape of the volume fraction distribution.

#### 3.1.3 Fourth-Degree Polynomial Distribution

To enable more sophisticated material distribution patterns, a fourth-degree polynomial function was implemented:

$$V(x,y) = a^1x^4 + a^2y^4 + a^3x^3y + a^4xy^3 + a^5x^2y^2 + a^6x^3 + a^7y^3 + a^8x^2y + a^9xy^2 + a^{10}x^2 + a^{11}y^2 + a^{12}xy + a^{13}x + a^{14}y + a^{15} \quad (21)$$

This higher-order polynomial provides greater flexibility in material distribution through fifteen independent coefficients.

#### 3.1.4 Sixth-Degree Polynomial Distribution

The most complex distribution pattern was achieved using a sixth-degree polynomial function:

$$V(x,y) = \sum_i a_i x^i y^j \; where \; i + j \leq 6 \quad (22)$$

This function includes 28 independent coefficients, offering the highest degree of freedom in controlling material distribution patterns.

For all distribution methods, the volume fraction values were normalized to ensure they remained within the physical bounds of $[0,1]$ across the entire plate domain. A $9 \times 9$ node distribution was implemented to accurately capture these material property variations across the panel.

### 3.2 Genetic Algorithm Optimization

The optimization process in this study employs a genetic algorithm $(GA)$, which is a metaheuristic optimization method inspired by natural selection principles. This approach is particularly suitable for optimizing the volume fraction distribution due to its ability to handle complex, non-linear problems with multiple variables.

The genetic algorithm operates on a population of potential solutions, where each individual represents a specific volume fraction distribution pattern. The fitness function, which evaluates the quality of each solution, is defined as:

$$F = w_1\left(\frac{\lambda}{\rho}\right) + w_2\left(\frac{T_{cr}}{\rho}\right) \quad (23)$$

Where:

$\lambda$ is the critical dynamic pressure, $T_{cr}$ is the critical temperature, $\rho$ is the material density, and $w_1, w_2$ are weighting factors to balance the importance of aerodynamic and thermal performance criteria respectively.

## 4. Application and Numerical Results

A higher-order quadrilateral element was employed to facilitate mesh convergence. Convergence studies involved progressively increasing both the number

of nodes per element (ranging from $3x3$ to $8x8$) and integration points. To quantify convergence, predicted post-buckling deflections and dynamic pressure responses were monitored. Sufficiently converged solutions were achieved using a $5x5$ node formulation with 9 Gaussian quadrature points for numerical integration [20], in the present study, a more refined $9x9$ node distribution was implemented for the volume fraction to ensure higher accuracy in each population capturing the material property variations across the panel. This enhanced mesh resolution allows for more precise representation of the various volume fraction distributions investigated, particularly beneficial for the higher-order polynomial distributions such as the fourth degree and sixth-degree cases.

*Table 1. Mechanical and thermal properties of Ni and Al constituents*

| Property | Nickel | Aluminum |
|---|---|---|
| **Modulus of Elasticity** $(E)$ | $22.4\,x10^{10}\ Pa$ | $7.1\,x\,10^{10}\ Pa$ |
| **Poisson's Ratio** $(\nu)$ | 0.31 | 0.3 |
| **Thermal Expansion** $(\alpha)$ | $9.92\,x10^{-6}\ /°C$ | $22.5\,x\,10^{-6}\ /°C$ |
| **Density** $(\rho)$ | $8900\ kg/m^3$ | $2700\ kg/m^3$ |

This section presents detailed numerical results and discussions on the aerothermal buckling response of functionally graded square plates. The analysis considers panel dimensions, airflow, and directions as illustrated in Figure 1. The panel is assumed to have fixed edges on all sides. Table 1 provides the material properties for individual constituents.

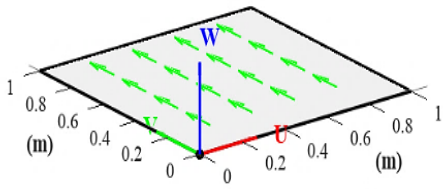


*Figure 1. Schematic of Panel Geometry Deformation.*

The optimization process employed 100 maximum generations with a population of 450 individuals. A subset of 150 individuals was utilized for specific computational strategies, enabling a comprehensive exploration of the design space and potential optimal solutions.

## 4.1 Material Properties and Performance Metrics

This investigation begins with establishing homogeneous Nickel as the reference material for performance comparison, characterized by a density of $8900\ kg/m^3$, critical dynamic pressure $(\lambda)$ of 852, and critical temperature of 0.336. To evaluate the effectiveness of various volume fraction distributions, performance metrics were established to measure relative changes $(\Delta)$ in density, critical dynamic pressure, and critical temperature compared to the reference case. Additionally, homogeneous Aluminum was included in the analysis to provide a benchmark for lightweight material performance, exhibiting a 70% reduction in density but accompanied by significant decreases in structural performance.

## 4.2 Volume Fraction Distribution Effects

Figure 2 illustrates the optimization distribution patterns for four different cases: linear distribution, quadratic distribution, 4th degree polynomial distribution, and 6th degree polynomial distribution. The 4th degree polynomial distribution demonstrates superior optimization performance as it effectively distributes the higher-density Nickel material in regions of maximum stress concentration, specifically at the center and corner midpoints of the plate.

This distribution pattern aligns optimally with the structural requirements by placing material where it's most needed for mechanical performance.

*Table 2 Mode Shape Values for Different Volume Fraction Distribution Functions (Hz).*

| Mode No. | 1st | 2nd | 3rd | 4th | 5th | 6th |
|---|---|---|---|---|---|---|
| **Linear** | 53.06 | 108.89 | 111.36 | 165.45 | 192.50 | 199.57 |
| **Quadratic** | 52.88 | 111.24 | 111.82 | 167.34 | 198.76 | 204.56 |
| **Polynomial 4 degree** | 53.73 | 109.62 | 115.05 | 171.70 | 197.44 | 202.26 |
| **Polynomial 6 degree** | 53.06 | 108.89 | 111.36 | 165.45 | 192.50 | 199.57 |

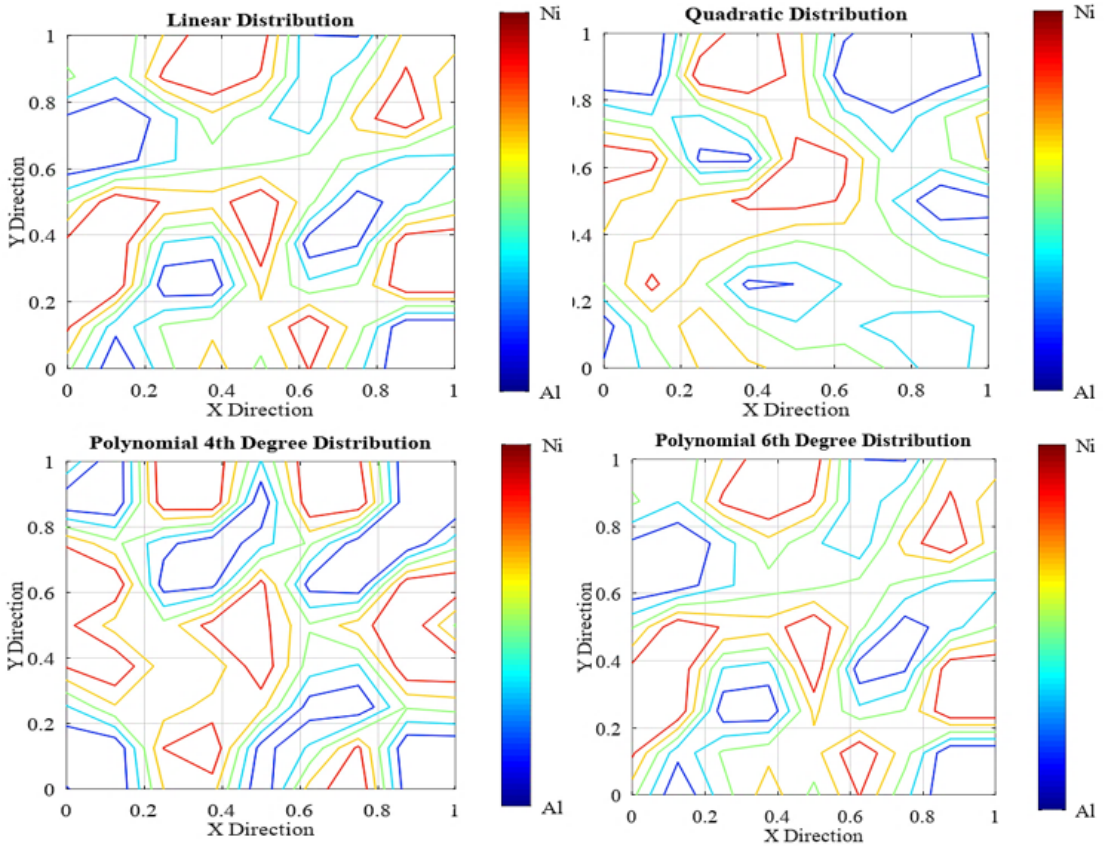


*Figure 2. Identification volume fraction with different Cases.*

The analysis of volume fraction distribution (Linear, Quadratic, 4th degree polynomial, and 6th degree polynomial) highlights the 4th degree polynomial as the most effective in enhancing the first mode shape values Table 2 and illustrated in Figure 3. This distribution demonstrates superior performance at critical positions, such as Mode 1 (53.73 Hz), Mode 3 (115.05 Hz) and Mode 4 (171.70 Hz), surpassing the values achieved by linear, quadratic, and 6th degree polynomial distributions. Its ability to optimize material properties across the structure contributes to these enhanced modal behaviors, resulting in improved dynamic stability and structural response.

The 4th degree polynomial strikes an optimal balance between complexity and effectiveness, avoiding the computational challenges of higher-degree polynomials while achieving better stiffness characteristics and resistance to dynamic loads. Notably, the 6th degree polynomial distribution yields result similar to the linear distribution, indicating diminishing returns with increasing polynomial degrees beyond the fourth order.

This reinforces the 4th degree polynomial's suitability as the optimal choice for dynamic performance improvement.

*Table 2 Mode Shape Values for Different Volume Fraction Distribution Functions (Hz).*

| Mode No. | 1st | 2nd | 3rd | 4th | 5th | 6th |
|---|---|---|---|---|---|---|
| **Linear** | 53.06 | 108.89 | 111.36 | 165.45 | 192.50 | 199.57 |
| **Quadratic** | 52.88 | 111.24 | 111.82 | 167.34 | 198.76 | 204.56 |
| **Polynomial 4 degree** | 53.73 | 109.62 | 115.05 | 171.70 | 197.44 | 202.26 |
| **Polynomial 6 degree** | 53.06 | 108.89 | 111.36 | 165.45 | 192.50 | 199.57 |

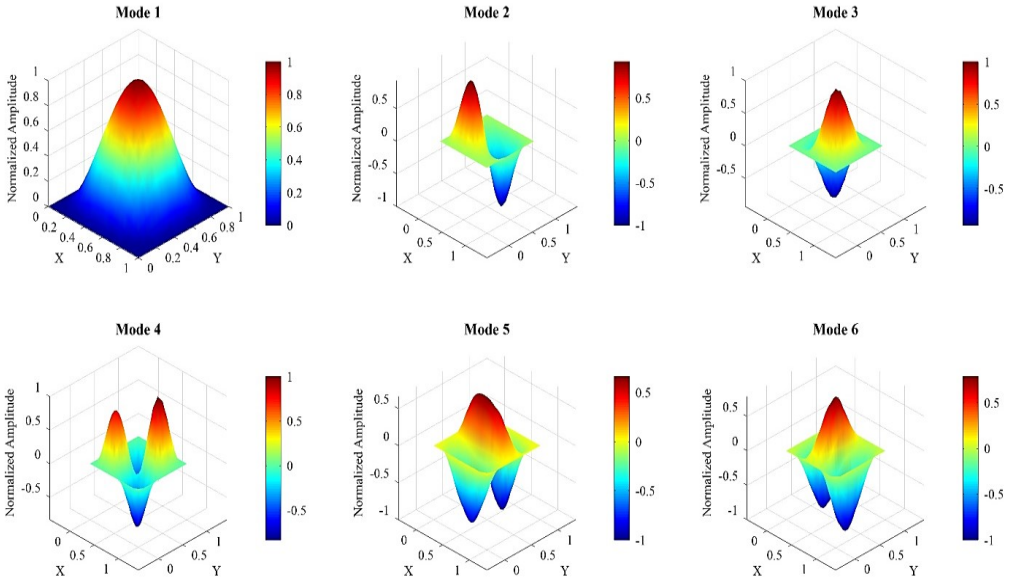


*Figure 3. Fist six mode shape for panel.*

### 4.3 Weight-Performance Relationship

The investigation of different volume fraction distributions revealed remarkable insights into the relationship between weight reduction and structural performance. The fourth-degree polynomial distribution emerged as the most efficient configuration, achieving a substantial 33% reduction in overall panel density (5990 Kg/m$^3$) compared to the homogeneous Nickel reference case. What makes this distribution particularly noteworthy is its ability to maintain structural integrity while significantly reducing weight. Despite the considerable decrease in density, the critical dynamic pressure only decreased by 19% relative to the reference case, demonstrating an optimal balance between weight savings and structural performance.

Other distributions, while also achieving weight reductions, showed less favorable performance characteristics. The linear distribution achieved a 40% weight reduction but suffered from a more substantial 31% decrease in critical dynamic pressure. Similarly, the quadratic distribution resulted in a 34% weight reduction with a 25% decrease in critical dynamic pressure, while the sixth-degree polynomial showed a 33% weight reduction but experienced a 27% decline in critical dynamic pressure.

#### 4.3.1 Critical Dynamic Pressure Analysis

The critical dynamic pressure analysis provides crucial insights into the structural stability of the functionally graded panel under various volume fraction distributions. The fourth-degree polynomial distribution demonstrated superior performance with a critical dynamic pressure value of 690, representing only a 19% reduction from the reference case while maintaining a significantly lighter structure. This notable achievement in maintaining structural integrity while reducing weight by 33% highlights the effectiveness of the fourth-degree polynomial distribution in optimizing the panel's design. The other distributions, while showing improvements, did not achieve the same level of efficiency. The linear distribution yielded a critical dynamic pressure of 590, the quadratic distribution achieved 641, and the sixth-degree polynomial resulted in 622, all showing larger relative decreases in performance compared to their weight reduction benefits provided in Table 3.

*Table 3. variance in aerodynamic pressure with density.*

| | Density (Kg/m3) | Best Fit Pressure | Non-Dimensional Pressure | Δ Density/ Density Ref. | Δ Non-Dimensional Pressure/ Pressure Ref. |
|---|---|---|---|---|---|
| **Homogeneous Nickel (Ref.)** | 8900 | 9.57 | 852 | 0% | 0% |
| **Homogeneous Aluminum** | 2700 | 9.96 | 269 | 70% | 68% |
| **Linear** | 5296 | 11.14 | 590 | 40% | 31% |
| **Quadratic** | 5870 | 10.92 | 641 | 34% | 25% |
| **Polynomial 4 degree** | 5990 | 11.52 | 690 | 33% | 19% |
| **Polynomial 6 degree** | 5923 | 10.50 | 622 | 33% | 27% |

*Table 4. variance in temperature with density.*

| | Density (Kg/m3) | Best Fit Temperature | Temperature(C) | Δ Density/ Density Ref. | Δ Temperature/ Temperature Ref. |
|---|---|---|---|---|---|
| **Homogeneous Nickel (Ref.)** | 8900 | 3.77 | 0.336 | 0% | 0% |
| **Homogeneous Aluminum** | 2700 | 5.52 | 0.149 | 70% | 56% |
| **Linear** | 5296 | 4.37 | 0.231 | 40% | 31% |
| **Quadratic** | 5870 | 4.05 | 0.238 | 34% | 29% |
| **Polynomial 4 degree** | 5990 | 4.29 | 0.257 | 33% | 23% |
| **Polynomial 6 degree** | 5923 | 4.17 | 0.247 | 33% | 26% |

### 4.3.2 Critical Temperature Analysis

The thermal performance of the functionally graded panel, characterized by its critical temperature behavior, represents another crucial aspect of the structural design.

The fourth-degree polynomial distribution demonstrated favorable thermal stability with a critical temperature of 0.257, showing a 23% change from the reference case. This thermal performance characteristic is particularly significant when considered alongside the substantial weight reduction achieved. The analysis revealed that other distributions exhibited varying degrees of thermal performance: the linear distribution showed a 31% change in critical temperature, the quadratic distribution demonstrated a 29% change, and the sixth-degree polynomial resulted in a 26% change. These results further support the overall superiority of the fourth-degree polynomial distribution in achieving an optimal balance between thermal stability and weight reduction provided in Table 4.

When comparing these thermal results with the structural performance metrics, it becomes evident that the fourth-degree polynomial distribution consistently provides the most favorable combination of properties. The ability to maintain thermal stability while achieving significant weight reduction and preserving structural integrity makes this distribution particularly attractive for practical applications where multiple performance criteria must be satisfied simultaneously.

## 4.4 Nonlinear Static Post-Buckling Behavior Analysis Without Aerodynamic Forces.

The analysis of nonlinear post-buckling behavior in plates without aerodynamic pressure is investigated through various material distributions. Table 5 presents a comparative study where homogeneous Nickel with density 8900 kg/m$^3$ and post-buckling to thickness ratio of 2.11 serves as the primary reference case. A secondary homogeneous Aluminum case with density 2700 kg/m$^3$ demonstrates a post-buckling to thickness ratio of 3.58, marking a significant 70% reduction in density from the Nickel reference while achieving enhanced post-buckling characteristics.

The implementation of polynomial distributions, as illustrated in Figure 4, reveals interesting patterns in structural response. The linear distribution achieves a 40% density reduction with a post-buckling ratio of 2.84, while the quadratic distribution shows a 34% density reduction with a 2.79 ratio. Notably, the fourth-degree polynomial distribution emerges as the optimal configuration, achieving a 33% density reduction with the most efficient post-buckling ratio of 2.77. The results demonstrate that increasing the polynomial degree beyond the fourth degree does not yield improved performance, as evidenced by the sixth-degree polynomial distribution, which reverts to behavior similar to the linear distribution with a 33% density reduction and a 2.84 post-buckling ratio.

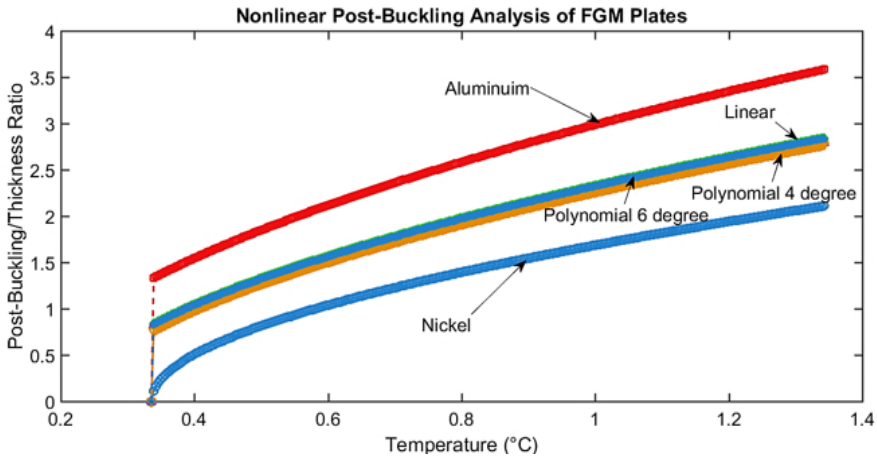


*Figure 4. Post-buckling deflection / Thickness of volume fraction distribution*

*Table 5. variance in nonlinear post-bucking deflection with density absence aerodynamic pressure.*

| | Density (Kg/m3) | Post-Buckling/ Thickness @ T=1.340 (C) | Δ Density/ Density Ref. | Δ Post-Buckling/ Post-Buckling Ref. |
|---|---|---|---|---|
| **Homogeneous Nickel (Ref.)** | 8900 | 2.11 | 0% | 0% |
| **Homogeneous Aluminum** | 2700 | 3.58 | 70% | 70% |
| **Linear** | 5296 | 2.84 | 40% | 35% |
| **Quadratic** | 5870 | 2.79 | 34% | 32% |
| **Polynomial 4 degree** | 5990 | 2.77 | 33% | 31% |
| **Polynomial 6 degree** | 5923 | 2.84 | 33% | 35% |

### 4.5 Nonlinear Dynamic Post-Buckling Behavior Analysis with Aerodynamic Forces.

The analysis of the dynamic nonlinear post-buckling behavior of FGMs plates under various volume fraction distributions is crucial for understanding their structural integrity and performance.

In this section, we focus on the 4-degree polynomial volume fraction distribution, which represents one of the four cases investigated in the broader study. The contour plot of the flutter mode, as shown in the Figure 5, provides valuable insights into the optimum post-buckling deflection characteristics of the FGMs plate with this distribution.

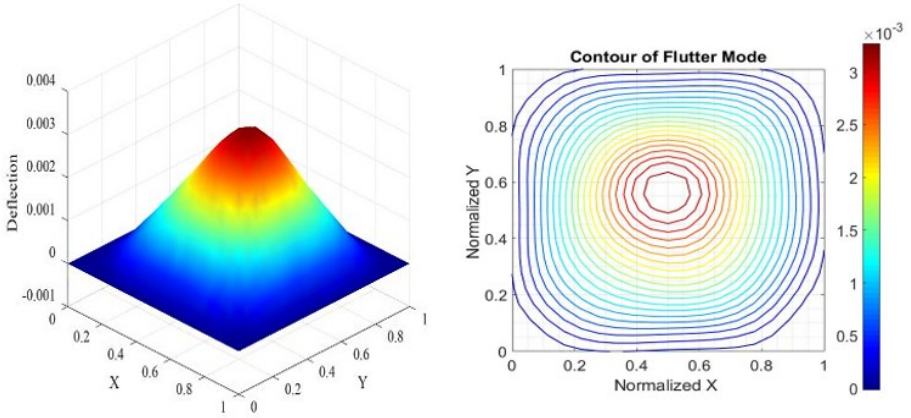


*Figure 5. Flutter mode for 4th degree polynomial distribution*

The central region of the contour plot indicates the area of optimal post-buckling deflection, where the normalized values are close to unity. This suggests that the plate exhibits the most desirable dynamic behavior when the deflection is concentrated near the center, in the direction of the applied aerodynamic loading. As the deflection moves away from the center, the normalized values decrease, indicating a less favorable dynamic response. This trend is evident in the concentric contour lines, which gradually decrease in value as the distance from the center increases.

The contour plot of the flutter mode for the 4-degree polynomial volume fraction distribution highlights the importance of the plate's structural configuration and material distribution in determining its dynamic nonlinear post-buckling behavior. The optimal post-buckling deflection occurs when the deformation is centered and aligned with the direction of the aerodynamic loading, as evidenced by the high normalized values in the central region of the plot. This information can be valuable in the design and optimization of FGMs plate structures to ensure their structural integrity and performance under dynamic loading conditions.

## 5. Conclusions

This study demonstrates the effectiveness of polynomial-based optimization for functionally graded materials in aerospace applications. Key findings include:

**A. Performance Optimization:**

- Achieved 33% weight reduction with only 19% decrease in critical dynamic pressure;
- Maintained structural integrity under combined thermal and aerodynamic loads;
- Demonstrated superior flutter resistance compared to traditional distributions.

**B. Methodological Innovation:**

- Identified 4th degree polynomial distribution as optimal for computational efficiency;
- Developed efficient approach for material distribution optimization;

- Established new benchmarks for FGM performance optimization.

**C. Practical Applications:**

- Direct implications for aerospace structural design;
- Potential for implementation in high-speed flight applications;
- Framework for future optimization studies.

## References


[1] Ibrahim, H.H., M. Tawfik, and M. Al-Ajmi, Thermal buckling and nonlinear flutter behavior of functionally graded material panels. Journal of Aircraft, 2007. 44(5): p. 1610-1618.

[2] Ibrahim, H.H., M. Tawfik, and M. Al-Ajmi, Non-linear panel flutter for temperature-dependent functionally graded material panels. computational mechanics, 2008. 41: p. 325-334.

[3] Shaker, A., et al., Stochastic finite element analysis of the free vibration of functionally graded material plates. Computational Mechanics, 2008. 41: p. 707-714.

[4] Sohn, K.-J. and J.-H. Kim, Nonlinear thermal flutter of functionally graded panels under a supersonic flow. Composite Structures, 2009. 88(3): p. 380-387.

[5] Ibrahim, H.H. and M. Tawfik, Limit-cycle oscillations of functionally graded material plates subject to aerodynamic and thermal loads. Journal of Vibration and Control, 2010. 16(14): p. 2147-2166.

[6] Ibrahim, H.H., et al., Thermo-acoustic random response of temperature-dependent functionally graded material panels. Computational Mechanics, 2010. 46: p. 377-386.

[7] Hussein, O.S. and S.B. Mulani, Multi-dimensional optimization of functionally graded material composition using polynomial expansion of the volume fraction. Structural and Multidisciplinary Optimization, 2017. 56: p. 271-284.

[8] Chu, F., et al., Buckling analysis of functionally graded thin plate with in-plane material inhomogeneity. Engineering Analysis with Boundary Elements, 2016. 65: p. 112-125.

[9] Gupta, A. and M. Talha, Recent development in modeling and analysis of functionally graded materials and structures. Progress in Aerospace Sciences, 2015. 79: p. 1-14.

[10] Jha, D., T. Kant, and R. Singh, A critical review of recent research on functionally graded plates. Composite structures, 2013. 96: p. 833-849.

[11] Kieback, B., A. Neubrand, and H. Riedel, Processing techniques for functionally graded materials. Materials Science and Engineering: A, 2003. 362(1-2): p. 81-106.

[12] Liew, K.M., X. Zhao, and A.J. Ferreira, A review of meshless methods for laminated and functionally graded plates and shells. Composite Structures, 2011. 93(8): p. 2031-2041.

[13] Almeida, S.R., G.H. Paulino, and E.C. Silva, Layout and material gradation in topology optimization of functionally graded structures: a global–local approach. Structural and Multidisciplinary Optimization, 2010. 42: p. 855-868.

[14] Bahadori, R. and M. Najafizadeh, Free vibration analysis of two-dimensional functionally graded axisymmetric cylindrical shell on Winkler–Pasternak elastic foundation by First-order Shear Deformation Theory and using Navier-differential quadrature solution methods. Applied Mathematical Modelling, 2015. 39(16): p. 4877-4894.

[15] Goupee, A.J. and S.S. Vel, Two-dimensional optimization of material composition of functionally graded materials using meshless analyses and a genetic algorithm. Computer methods in applied mechanics and engineering, 2006. 195(44-47): p. 5926-5948.

[16] Aragh, B.S., et al., A novel 2-D six-parameter power-law distribution for free vibration and vibrational displacements of two-dimensional functionally graded fiber-reinforced curved panels. European Journal of Mechanics-A/Solids, 2011. 30(6): p. 865-883.

[17] Xia, L. and P. Breitkopf, Design of materials using topology optimization and energy-based homogenization approach in Matlab. Structural and multidisciplinary optimization, 2015. 52(6): p. 1229-1241.

[18] Xia, Q. and M.Y. Wang, Simultaneous optimization of the material properties and the topology of functionally graded structures. Computer-Aided Design, 2008. 40(6): p. 660-675.

[19] Zhou, M., J. Xi, and J. Yan, Modeling and processing of functionally graded materials for rapid prototyping. Journal of Materials Processing Technology, 2004. 146(3): p. 396-402.

[20] Fayed, M.E., et al. Modelling and Parametric Study for Panel Flutter Problem using Functionally Graded Materials. in Journal of Physics: Conference Series. 2024. IOP Publishing.

[21] M. Tawfik 2018 In Search for the Super Element: Algorithms to Generate Higher Order Elements ResearchGate [Online] DOI: 10.31142/ijtsrd18565.

[22] M. Tawfik 2021 Panel Flutter ResearchGate [Online] DOI:10.13140/RG.2.1.1537.6807.